Impact of H_2/CH_4 blends on the flexibility of micromix burners applied to industrial combustion systems

G. Lopez-Ruiz [a], I. Alava [b], J. M. Blanco [c]

[a] *Basque Center for Applied Mathematics (BCAM), Alameda Mazarredo 14, 48009, Spain.*
[b] *Ikerlan Technology Research Centre, Basque Research and Technology Alliance (BRTA). P.º J.M. Arizmendiarrieta, 2. 20500 Arrasate/Mondragón, Spain.*
[c] *Energy Engineering Department, School of Engineering, Building I, University of the Basque Country, UPV/EHU, Plaza Ingeniero Torres Quevedo s/n, 48013 Bilbao, Spain*

Abstract

The present paper investigates the feasibility of using H_2/CH_4 fuel blends in micromix-type burners applied to industrial combustion systems. The micromix burner concept, characterised by the formation of miniaturised and compact turbulent diffusion flames, was developed for gas turbine hydrogen burners showing low NO_x emissions (below 10 ppm) without flashback risk, which represent the main issues when using pure hydrogen or hydrogen enriched natural gas blends as fuel, making it a promising concept to be applied in industrial burners. The study was carried out through numerical CFD simulations, accounting for detailed chemistry calculations of turbulent micromix flames and previously validated through experimental measurements in a laboratory-scale micromix burner prototype. The resulting flow, temperature and exhaust emission characteristics for three H_2/CH_4 fuel blends with H_2 content of 90, 75 and 60% respectively were analysed and discussed for air-fuel equivalence ratios at λ =1.8 and 1.6 (lower than the well-characterised air-fuel equivalence ratios in micromix gas turbine burners at λ =2.5 and closer to current industrial burners), considering an energy density of 14 MW/m^2 bar. Numerical results showed low fuel flexibility for industrial-scale micromix burners, with still low NO_x emissions (12-85 ppm) but relatively high CO emissions (448-4970 ppm) for the considered blends and λ values. The lowest CO emissions were given together with jet penetration phenomena, ruling out the feasibility of these design points due to the greater importance of the latter phenomenon.

Key words: Micromix combustion, Hydrogen burners, Low NO_x, Alternative fuels, Industrial burners, Industrial combustion, Combustion modelling

Nomenclature

Latin characters

D_{H_2}	Hydrogen jet diameter [mm]
k	Turbulence kinetic energy [m^2/s^2]
$\dot{m}_{air}$	Air mass flux [kg/s]
r_m	Momentum-flux ratio [-]
V_{air}	Air velocity [m/s]
V_{H_2}	Hydrogen velocity [m/s]
y_{H_2}	Injection depth [mm]

Greek characters

λ	Air excess [-]
ω	Specific dissipation rate [1/s]
ρ_{Air}	Air density [kg/m^3]
ρ_{H_2}	Hydrogren density [kg/m^3]

Abbreviations

ED	Energy Density [kW/dm^2]
EDC	Eddy dissipation concept
FGM	Flamelet generated manifold
IB	Industrial burner
MCP	Micromix combustion principle

1. Introduction

The quest for energy system decarbonization is becoming a priority, where green hydrogen appears as an energy vector to deal with the intermittent and distributed nature of the increasing renewable and non-renewable power plants [1, 2, 3]. Once generated and stored, gaseous hydrogen could be used in several applications. In this context, greenhouse and pollutant emissions from industrial combustion systems could be reduced by using pure hydrogen or hydrogen/natural gas blends as fuel in such combustion devices.

Among others, green hydrogen has become a promising alternative to conventional fossil fuels to reduce the overall emissions in different sectors [4, 5, 6, 7]. It can be generated through water electrolysis and other renewable methods, using the energy excess in low demand periods and storing it to be afterwards used in different applications, acting as an energy vector. In that sense, the rising price of natural gas and conventional fossil fuels in 2022 due to the high energetic dependence of the EU countries, the unstable socio-economic context after the COVID pandemic and the climate emergency that we are experiencing, have raised a problem of global dimensions in which the development of new and more sustainable technologies will have to go together with a drastic change in our way of thinking and new organisational forms in the direction of degrowth [8, 9].

Thus, green hydrogen, together with many other technologies, is one of the alternatives that can fit into a new energy model. In order to develop this technology, the European Clean Hydrogen Alliance was set up by the Commission in July 2020 to support the creation of a European hydrogen industry, bringing together over 1500 stakeholders, which shows the evident commitment that is being made to this technology [10]. It is worth to mention that the current context will inevitably accelerate these efforts by the commission and its member countries.

The use of hydrogen/natural gas blends in combustion systems is in the spotlight and is one of the most immediate alternatives for CO_2 reduction in gas-fired combustion systems as it could offer several advantages in terms of flexibility and optimum profit of the resources [11, 12]. However, several challenges arise not only from the combustion process itself [13, 14], but from the upstream gas blending supply, requiring detailed studies depending on the location and taking into account renewable capacity, hydrogen demand and other variables affecting logistics and storage [15]. According to the technical report presented by J.Bard *et al.* [16], H_2-blendings of 20 (vol.%) seems to be technically feasible in a mid-term perspective. Their results showed that replacing 20 (vol.%) natural gas by H_2, the energy flow is decreased by ca. 13 (vol.%), leading to approximately 6-7 % GHG-savings. They concluded that the physical supply of 100% H_2 has advantages and could still allow for approaches such as gradual on-site blending. However, they highlighted that H_2 usage should be limited to areas where it is needed and cannot be substituted by electricity, leaving open the question of how to transport the produced hydrogen to the end-users.

Despite the mentioned uncertainties, in order to reduce the greenhouse emissions and also the dependence on natural gas, combustion devices should be substituted or adapted to burn 100% hydrogen or H_2 blends above 20 (vol.%), specially in those applications where electrification is not possible, e.g. melting furnaces. In this context, the present paper focuses on the use of hydrogen-enriched natural gas mixtures in micromix-type industrial burners, which differ from micromix-type gas turbines due to differences in operating conditions as highlighted in our previous study [17]. The choice of this type of burner will be further explained below. Moreover, since the study focuses on the combustion process, isolating the burner and avoiding the interaction with the target load, the term industrial burner used in the present paper covers the whole family of burners that might be used in steam boilers, furnaces or different heat treatment processes, offering a broader analysis without closing itself off to a specific application.

In addition to the technical challenges of the fuel blending supply system outlined above, the combustion characteristics of hydrogen and hydrogen/natural gas blends presents several particularities. Among others, hydrogen presents a wide flammability limit in air (4-75 vol%), low ignition energy in air (0.019 mJ), low density (0.0899 kg/m^3) and high adiabatic flame temperature (2380 K) [18, 19]. In that sense, non-premixed burners, which are commonly used in industrial burners and gas turbine combustors, are preferable since they ensure safer operating conditions avoiding flashback and explosion risk when fuelled completely by hydrogen. However, this type of flames react at near stoichiometric conditions, resulting in near-adiabatic flame temperatures and consequent increase in thermal NO_x formation [20, 21]. Therefore, the main techno-

logical challenge concerning the design of hydrogen burners is to maintain both a high hydrogen fuel content under safe operating conditions and acceptable levels of thermal NO_x emissions.

In the non-premixed or diffusion combustion technology field related to the industrial sector and considering hydrogen as fuel, the micromix combustion principle (MCP) appears as a novel technology able to minimise the negative impacts derived from the hydrogen combustion. The combination of the jet crossflow principle with multiple injectors is the basis of the MCP as shown in Figure 1 (a). Thus, the fast mixing between reactants reduces the residence time of NO_x precursors [22, 23] generating miniaturised turbulent diffusion flames separated each other and stabilised between inner and outer vortices. The main design elements characterising the architecture of a micromix burner prototype with two hydrogen segments are depicted on Figure 1 (b). It must be noted that the number of segments and the final arrangement (linear or concentric rings) depend on the burner integration space and the desired energy density.

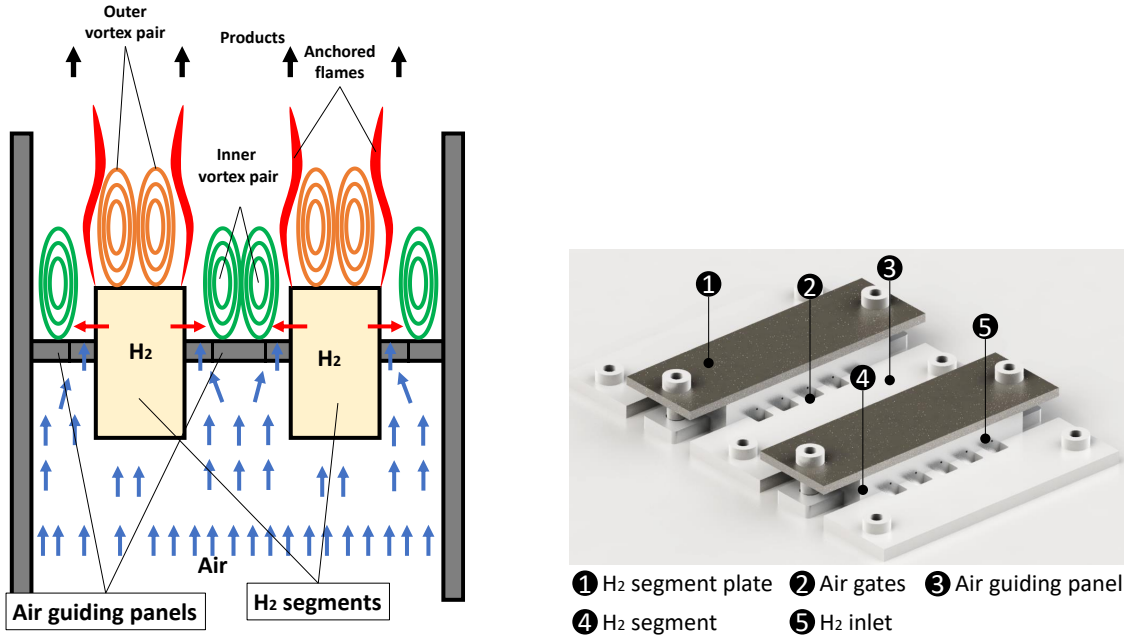

(a) (b)

Figure 1: (a) Scheme of the MCP (b) Micromix burner prototype [17]

In recent years, a huge amount of literature has been published on low NO_x MCP, carried out by Aachen University for Applied Sciences, B&B-AGEMA GmbH and Kawasaki Heavy Industries [22, 23, 24]. Moreover, research groups from Cranfield University have focused their attention towards hydrogen fuelled MCP aero-engines through the European Research project ENABLE H_2 [25, 26, 27].

Extensive studies exist on the flexibility of NG/H_2 blends in different types of burners and applications, focused on thermal NO_x, CO and CO_2 emissions, flame stability (premixed and partially-premixed systems) and air to gas ratio control systems [28, 29, 30, 31]. In particular, Fuel-flexibility of micromix gas turbine burners at high air-fuel equivalence ratios (represented by λ) with $\lambda > 2$ was studied by N.Beckmann [32] focusing on the burner geometry optimisation to keep the main micromix combustion characteristics and low emission levels along with high combustion efficiency for the widest possible range of H_2/CH_4 blends. Furthermore, the technical report presented by N.Tekin *et al.* [33] showed a real fuel-flexible micromix gas turbine in Kobe (Japan), being able to operate with 100% natural gas, NG/H_2 blends and 100% H_2.

Thus, the main purpose of the present paper is to analyse the feasibility of extrapolating the MCP for gas turbine burners to industrial-scale burners and study the fuel flexibility that was already developed for gas turbine operating conditions. For that purpose, a set of numerical simulations were carried out to assess the impact of different operating conditions at lower air-fuel equivalence ratios and different fuel blends at

atmospheric pressure conditions. The employed modelling approach was validated in our previous work [17] using a laboratory-scale micromix burner prototype.

The paper is structured as follows: Section 2 defines the objectives and justifies the selection of the variables to be studied. It also refers to the previous work on which the present study is based. Section 3 describes the combustion and turbulence models used as well as the most relevant aspects of the modelling. The geometry and the simulation domain are also presented. Section 4 describes the experimental setup where the measurements were carried out previously, using pure hydrogen as fuel, and which served to validate the modelling process. Section 5 presents the results of the simulations carried out for H_2/CH_4 blends at different λ values and studies the flexibility of the proposed burner geometry. The paper ends with the conclusions, which summarise the most relevant results, the different uncertainties and next steps.

2. Objectives and methodology

In contrast to the mentioned well established micromix burner design points, using hydrogen, hydrogen-syngas and hydrogen-methane mixtures [32, 34], the present paper investigates the feasibility of the micromix combustion principle (MCP) for industrial scale burners, which operate with lower air-fuel equivalence ratio (λ) levels and different power densities under atmospheric pressure [17, 35, 36].

H_2/CH_4 blends with H_2 content of 90, 75, and 60% have been considered respectively based in the Wobbe Index to ensure good interchangeability [32]. Reduced λ levels have been considered at λ=1.8 and 1.6, which are closer from current natural gas burner design points at λ =1.3 [36]. Furthermore, energy density (ED) was adapted to 14 MW/m^2 under atmospheric pressure in contrast to the energy densities studied in previous literature at 40-65 MW/m^2 under pressurised combustors with $P_{ref} \sim 6.5$ bar [23, 32]. Table 1 summarises the properties of the employed fuel blends depending on the hydrogen content and the λ value. Labels A and B followed by the percentage of hydrogen are used to distinguish the cases and refer to the results as will be seen below. As can be seen, the heating value by volume decreases for higher hydrogen percentages in the fuel. To maintain a constant power density (since the same energy output is required despite varying the fuel mixture), it is necessary to increase the volumetric flow rate of hydrogen and reduce that of methane, as shown in the last column (volumetric flow rate ratio).

Table 1: Classification of the simulated cases depending on the hydrogen content and λ value with the corresponding LHV and inlet volumetric flow percentages

	H_2 [vol.%]	λ [-]	LHV [MJ/m^3]	Q_{H_2}/Q_{CH_4} [-]
A60	60	1.6	2082	1.5
A75	75	1.6	1705	3
A90	90	1.6	1328	9
B60	60	1.8	2082	1.5
B75	75	1.8	1705	3
B90	90	1.8	1328	9

Figure 2 summarises the previous research stages, which served as basis for the present work (1-2) [17], together with the research steps covered in the present study (3-4) and the future steps that are expected to be taken (5). Thus, in order to achieve the desired energy density value at 14 MW/m^2 at λ, the present burner geometry was scaled, simulated and validated using pure hydrogen as described in our previous work [17]. These research stages correspond to points 1 and 2 in the flow diagram from Figure 2. On the basis of the resulting geometry, the fuel flexibility of micromix burners under the described industrial-scale burner conditions was investigated. As mentioned above, the scaling of the geometry was done for 60% H_2 on CH_4, (point 3 in the diagram) which fixes specific inlet diameters and dimensions of the burner to maintain the micromix combustion characteristics. Now the question is whether increasing the percentage of H_2 will maintain these characteristics or not. This stage corresponds to point 4, which is treated in the

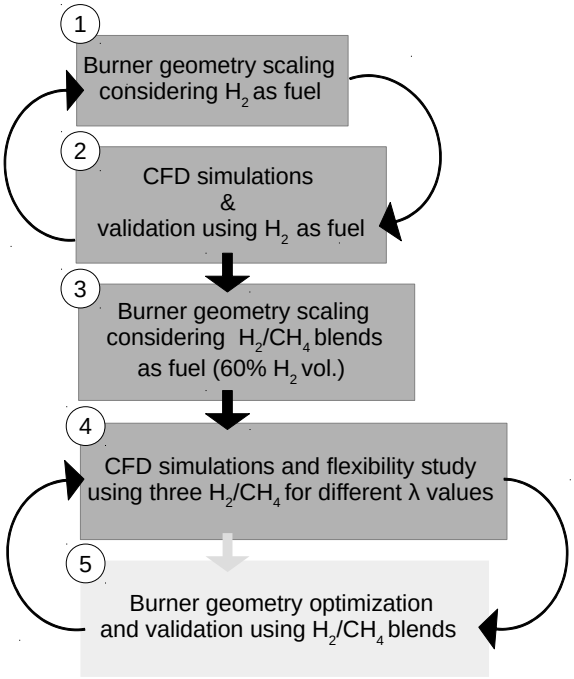

Figure 2: Flux diagram showing the research stages in the design of a micromix industrial burner for H_2/CH_4 blends.

present paper. Finally as future work, it is expected that the simulations will serve as basis for the geometry optimisation (point 5), with the aim of increasing the flexibility of the burner while ensuring low emissions of NOx, CO and CO2 as will be discussed in the conclusions.

It must be noted that in contrast to conventional natural gas burners, micromix burners would offer not only safe operating conditions without flashback risk and low NO_x emissions when using H_2/CH_4 blends as fuel, but also much shorter flame lengths, leading to smaller combustion chambers and more compact designs. In that sense, the main purpose of the present work is to demonstrate that low NO_x values are maintained for the re-defined operating conditions. Similarly, CO and CO_2 emissions will be also analysed as they will be crucial in assessing the fuel flexibility of the present micromix burner.

3. CFD Modelling

The steady three dimensional flow field was obtained by solving the Reynolds-averaged Navier-Stokes equations. The numerical domain is the same as that presented in our previous work [17], where a grid independence study was carried out leading to a final mesh with 1,200,000 cells. The general and detailed views of the domain are presented in Figure 3.

The present RANS calculations were performed using the k - ω SST turbulence model of Menter [37] following the same approach as in previous studies [38, 39]. The model has the benefits of the k - ω model in the inner boundary layer and also those offered by the k - ϵ model in the outer region. To avoid the use of wall functions and reduce uncertainty, the grid size for such zones was refined calculating the height and number of thin layers needed to solve the viscous sub-layer and ensure $y^+ \simeq 1$.

The steady transport equations for turbulent kinetic energy k and the specific dissipation rate ω are given in Eq. (1) and (2) respectively.

$$\frac{\partial(\rho u_j k)}{\partial x_j} = P - \beta^* \rho \omega k + \frac{\partial}{\partial x_j}\left[(\mu + \sigma_k \mu_t)\frac{\partial k}{\partial x_j}\right] \quad (1)$$

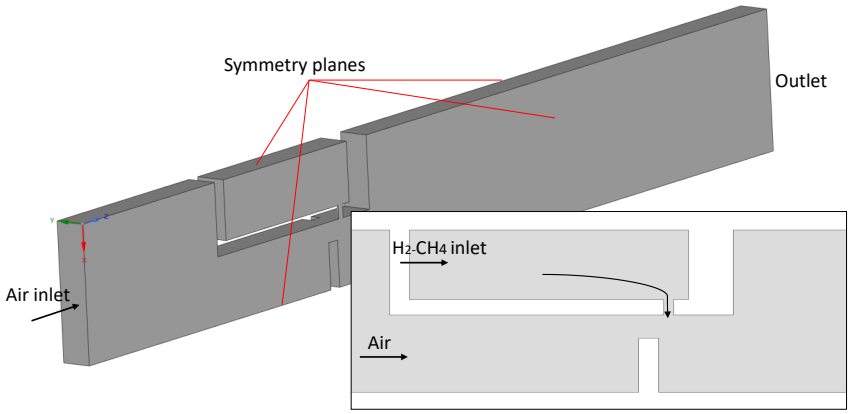

(a)

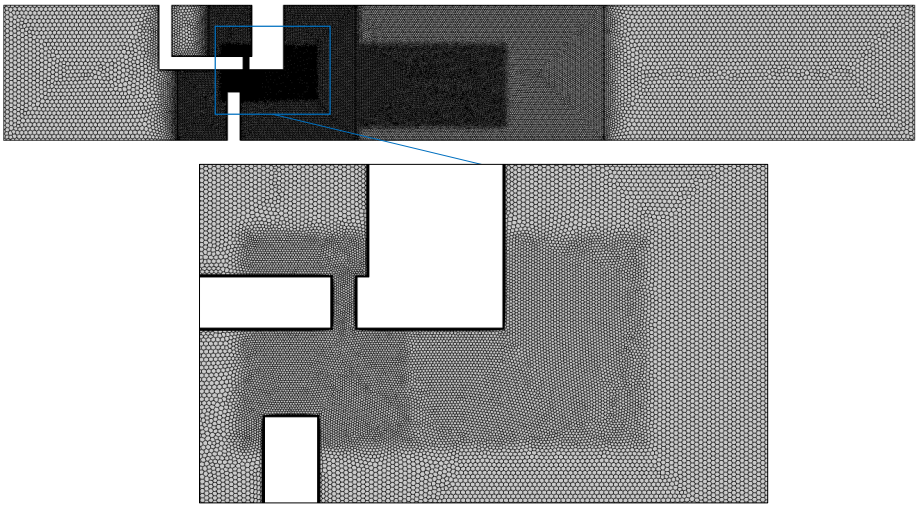

(b)

Figure 3: Numerical domain [17]

$$\frac{\partial(\rho u_j \omega)}{\partial x_j} = \frac{\gamma}{\nu_t} P - \beta \rho \omega^2 + \frac{\partial}{\partial x_j}\left[(\mu + \sigma_\omega \mu_t)\frac{\partial \omega}{\partial x_j}\right] + 2(1 - F_1)\frac{\rho \sigma_{\omega 2}}{\omega}\frac{\partial k}{\partial x_j}\frac{\partial \omega}{\partial x_j} \tag{2}$$

Furthermore, species transport equations including the chemical reaction term and energy conservation equation were also solved considering an incompressible ideal-gas mixture. The reaction source term was calculated through the so-called Eddy Dissipation Concept (EDC) model, which incorporates the influence of finite rate kinetics and the influence of turbulent fluctuations on mean chemical reaction rate. Moreover, the model solves a transport equation for the mass fractions Y_i of each specie i in the mixture (eq. (3)), being able to capture complex differential diffusion effects which could play an important role in hydrogen flames due to the high diffusivity of H_2 and are still difficult to represent by flamelet-based models [40].

Although the FGM model used in our previous work gave good results in terms of NO_x, in this case it

was decided to work with the EDC model to reduce the potential sources of error produced by flamelet-based combustion models and properly calculate CO formation, since the source terms responsible for the burn out of CO cannot be described by flamelet [41, 42]. Therefore, the only difference with respect to our previous numerical approach in [17] is in the combustion model, which in this case is improved as the EDC model offers more realistic solutions by reducing the uncertainties derived from the flamelet assumptions despite the increase in computational cost.

$$\frac{\partial(\rho Y_i)}{\partial t} + \nabla \cdot (\rho \mathbf{u} Y_i) = -\nabla \cdot J_i + \widetilde{\dot{\omega}_i} \tag{3}$$

This model is based on the turbulent energy cascade, assuming that the larger eddies loss their energy breaking into smaller eddies. The key assumption in the EDC model is that chemical reactions involved in a turbulence flow take place in those fine scales, which are locally treated as adiabatic, isobaric, Plug Flow Reactor (PFR). Based in the development of Magnusen [43], the mean reaction source term is defined as:

$$\widetilde{\dot{\omega}_i} = \frac{\bar{\rho}(\xi^*)^2}{\tau^*[1-(\xi^*)^3]}(Y_i^* - \widetilde{Y_i}) \tag{4}$$

Where ξ^* and τ^* represent the size of the fine structure and the mean residence time, defined by means of local viscosity, turbulent kinetic energy and its dissipation rate. Here, Y_i^* represents the species mass fraction calculated from the current value $\widetilde{Y_i}$ by means of the considered reaction mechanism over the time scale τ [44]. The integration of the Arrhenius reaction rates in the fine structures was carried out considering the reaction data from the widely used and validated DRM-22 [45] mechanism, consisting of 24 species and 104 reversible reactions. It must be also noted that ideal-gas-mixing law was used to compute the thermal conductivity and viscosity of the gas mixture. Assuming that the relative mass flux due to molecular diffusion is governed by a Fick's law, mass diffusivity was calculated through the mixture-averaged approach.

Finally, since NO_x models are commonly decoupled from the main reaction mechanism, the reaction rates from the well-known thermal NO_x Zeldovich mechanism were computed in a post-processing step using the converged temperature and species concentration values [17, 21]. The calculation was carried out solving the transport equation for Y_{NO}:

$$\nabla \cdot (\rho \mathbf{u} Y_{\mathrm{NO}}) = \nabla \cdot (\rho D \nabla Y_{\mathrm{NO}}) + \rho \dot{\omega}_{\mathrm{NO}} \tag{5}$$

Here the reaction term $\dot{\omega}_{\mathrm{NO}}$ was calculated considering the Zeldovich mechanism:

$$O + N_2 \leftrightarrows N + NO \tag{6}$$
$$N + O_2 \leftrightarrows NO + O \tag{7}$$
$$N + OH \leftrightarrows NO + H \tag{8}$$

The presented NO_x values were calculated in the burner outlet and corrected to 15% O_2 on a dry basis [23].

Finally, it is worth noting that the commercial software ANSYS Fluent 2020R1 [46] was used in a computational cluster of parallel Intel Xeon Gold processors.

4. Experimental validation

It should be noted that this modelling and NO_x prediction approach was experimentally validated in our previous work [17] using a laboratory-scale micromix burner prototype shown in Figure 5. In order to check the correct operation of the burner and detect possible problems in the assembly of the setup, initial ignition tests were carried out without combustion chamber. Since hydrogen flames are almost invisible to the human eye, two filaments of silicon carbide (diameter 0.1 mm) were located at two different heights downstream the burner. Hence, in presence of flame, the filaments would heat up emitting detectable infrared radiation. As shown in Figure 4 (a), the initial tests verified the presence of micromix flames in the expected locations.

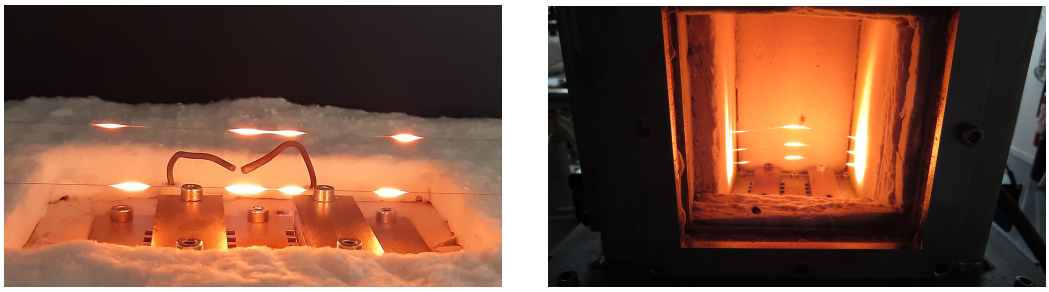

(a) (b)

Figure 4: Ignition tests. (a) without combustion chamber (exposed to the open air) (b) within the combustion chamber

Furthermore, the filaments were moved along the burner to check the correct ignition of the flames. The spark plug can be also identified in Figure 4 (a), which is necessary to start the combustion process. The electrodes were located downstream the last flames in the array, to avoid as far as possible their interaction with the main flow field.

Afterwards, the same procedure was followed confining the micromix burner into the combustion chamber. Figure 4 (b) shows the symmetric formation of the micromix flames in both parts of the hydrogen segments. As observed, an additional filament was added to ensure their presence throughout the test, as they are more prone to splitting due to their mayor exposure to thermal and fluid impacts and therefore greater weakness.

After ignition tests, thermal NO_x emissions were measured in the scaled prototype, characterised with a density of 50 kW/dm^2 and using pure hydrogen as fuel. Three design points were defined at reduced λ (λ =2, 1.8 and 1.6), showing good agreement with the numerical results.

The layout of the experimental setup is shown in Figure 5. Accordingly, hydrogen and air were supplied from a high pressure steel bottle and a compressed air line respectively. Hydrogen was introduced using two independent inlet pipes (3) as indicated in Figure 5 (a). Similarly, air was introduced from the bottom part of the prototype (1). Hydrogen and air mass flows were fixed through calibrated mass flow controllers connected to a Brooks 0152 Microprocessor control&read out unit. Emission measurements were carried out in the exhaust tube (7) using the Eco Physics CLD 60 NO_x detector once cooled in the heat exchanger (6). Table 2 summarises the most relevant characteristics of the presented measurement instrumentation.

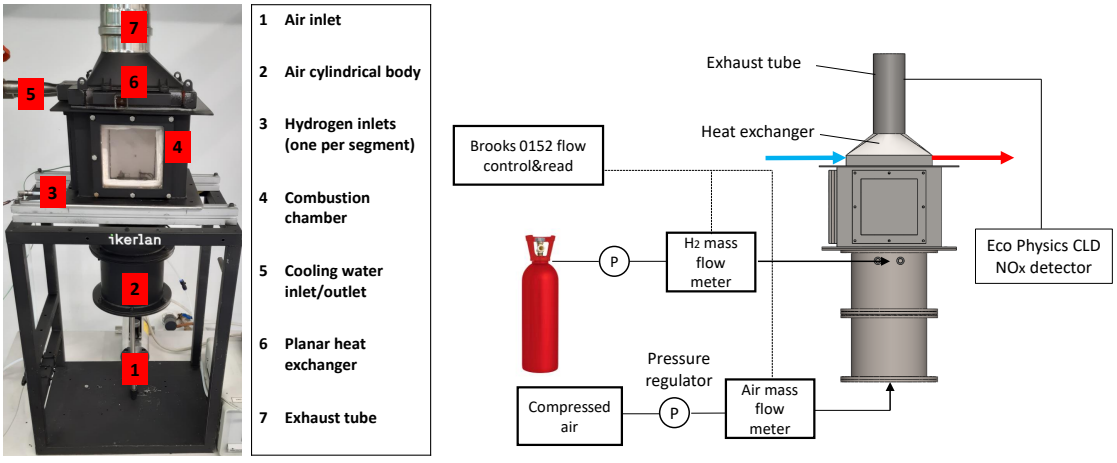

(a) (b)

Figure 5: Layout of the experimental setup showing the main components. (a) Real view (b) Schematic view

Table 2: Precision and range/capacity of the employed measurement instrumentation

Instrument	Precision	Range/Capacity
H_2 mass flow controller	±1.5 %	0-200 l/min
Air mass flow controller	±1.5 %	0-900 l/min
ECO Physics CLD	±0.1 ppm	0-200 ppm

Table 3: Comparison between numerical and experimental NO_x [ppm] concentrations at 50 kW/dm^2

	λ =2	λ =1.8	λ =1.6
Experimental	15.2	23.7	38.9
CFD	15.7	23.1	35.4
err. rel (%)	3.3	2.5	8.9

Experimental and numerical results of thermal NO_x emissions (corrected to 0% of O_2) using pure hydrogen as fuel at three λ levels are shown in Table 3. The higher error at λ=1.6 could be due to the lower turbulence level induced by the incoming air flow affecting the employed turbulent combustion model, which is developed for high levels of turbulence. Thus, the lower turbulence levels increased the uncertainties related to the combustion model and the prediction of the thermochemical variables. In addition, the lowest error at λ=1.8 may be related to the joint effect of both numerical and experimental uncertainties. Nevertheless, the relative error remained low in all three cases, supporting the potential of the selected modelling approach to estimate thermal NO_x formation.

The reliability of the validated numerical approach establishes a basis for simulations with new fuel blends as in the present work, showing the advantage of CFD simulations for predicting the influence of new design variables and saving experimental costs. As will be highlighted below, after the present modelling stage, it will be necessary to optimise the geometry and validate future simulations by means of an experimental setup including H_2/CH_4 blends.

5. Results and discussion

Temperature contours and velocity streamlines at each λ level are presented in Figure 6. In order to improve the understanding of the numerical outcomes, results at air-fuel equivalence ratios λ =1.6 and 1.8 were named with "A" and "B" respectively while hydrogen concentrations in the fuel were represented with numbers. Hence, six results will be analysed: A60, A75, A90 and B60, B75 and B90 as indicated in Figure 6. As mentioned, for a given λ level, higher hydrogen concentrations in the incoming fuel led to a higher fuel jet penetration into the air crossflow. This phenomena is characterised by the momentum flux ratio, which defines the relation between the fuel jet and the air cross-flow momentum, determining the injection depth of the former into the air cross-flow as [23]:

$$r_m = \frac{\rho_{fuel} V_{fuel}^2}{\rho_{Air} V_{Air}^2} = \frac{\frac{\dot{m}_{fuel}^2}{\rho_{fuel} A_{jet}^2}}{\frac{\dot{m}_{air}^2}{\rho_{air} A_{air}^2}} \tag{9}$$

Here the velocity of fuel has been expressed in terms of the inlet mass flow $\dot{m_{fuel}}$, jet area A_{jet} and fuel density ρ_{fuel}. Accordingly, higher hydrogen concentrations in the fuel reduced its density and the mass flow (for a given ED), increasing the momentum flux ratios and therefore promoting the jet penetration into the cross flow. Higher hydrogen concentrations in the fuel also reduces the air mass flow for a given λ, also promoting the jet penetration.

As indicated, the fuel jet penetration phenomena was observed in both λ levels, showing higher vortex temperatures caused by the burning process of the air-fuel mixture in such recirculating zone. This also led

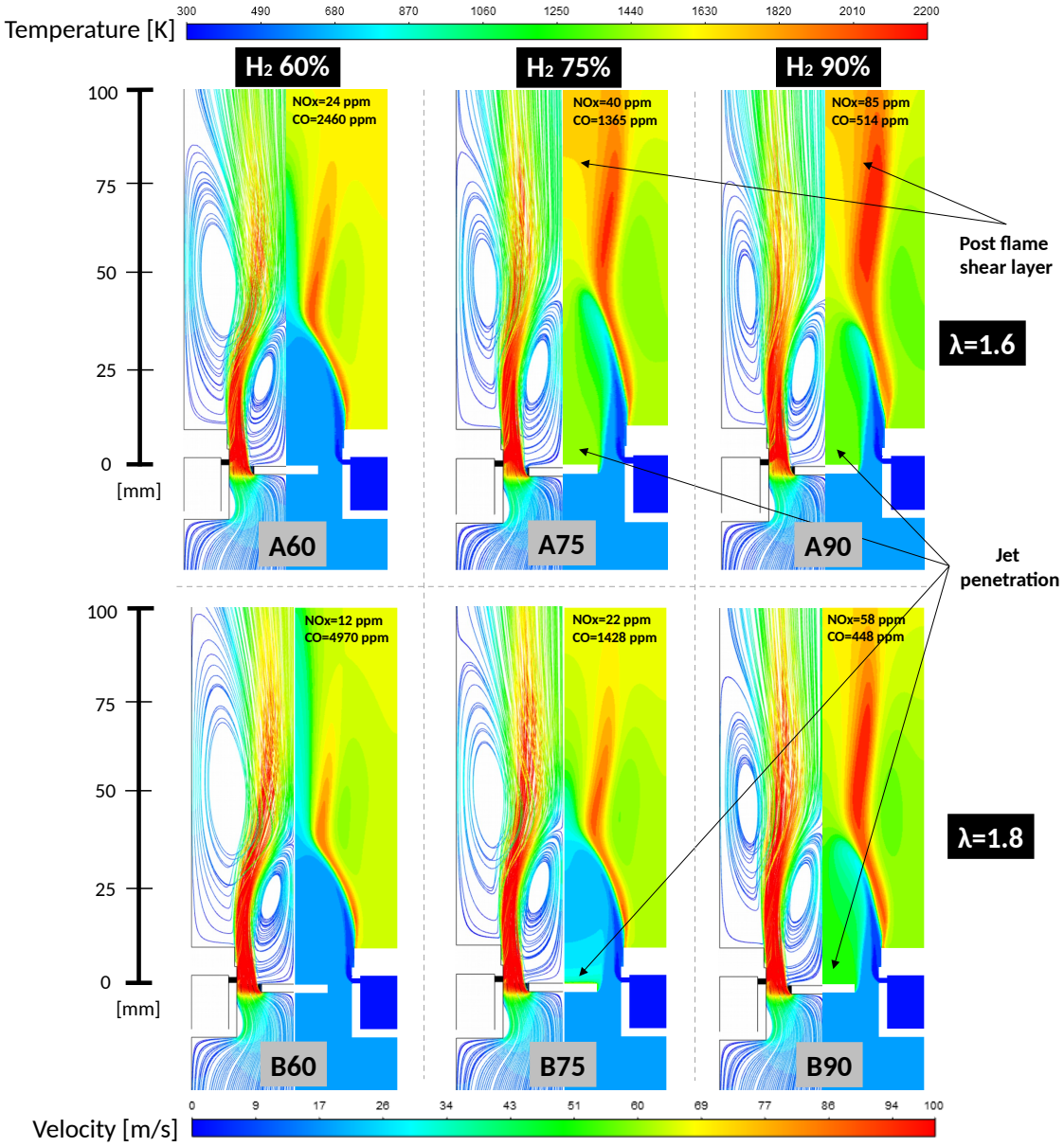

Figure 6: CFD results showing temperature contours and velocity streamlines in each case. NO_x and CO concentrations measured in the domain outlet and measured to 0% O_2 are also included

to a higher temperatures in the air guiding panel surface that could cause irreversible damages due to the high thermal impact on the burner material [32].

Concerning the nitrogen oxide emissions, numerical results showed that most of the NO_x was produced by the thermal NO_x formation mechanism (more than 95% percent) against the NO_x production by the prompt-NO_x mechanism. It can be see that low NO_x values were maintained below 30 ppm for A60, B60 and B75. In these cases, the order of magnitude of the NO_x concentrations remained at similar levels of the experimental values shown in Table 3. In contrast, the higher NO_x concentrations above 30 ppm at

A75, A90 may be explained by combination of the post shear layer formation phenomena and the worse mixing in the jet cross-flow zone due to the jet penetration. On the other hand, no shear layer was observed at B90, concluding that the higher NO_x concentrations were caused by the worse mixing. Figure 7 (a) shows that NO_x formation was concentrated in the post shear layer flame zone for A75 and A90, caused by the worse mixing in the jet cross-flow. This led to the combustion of the remaining fuel fraction in such zones, increasing the overall height of the flame and promoting the formation of the post shear layer flame fraction. In contrast to A90, the NO_x fractions for B90 were located in the near flame due to the lack of post shear-layer formation, which may be attributed to the higher air dilution and lower combustion product temperatures at λ =1.8.

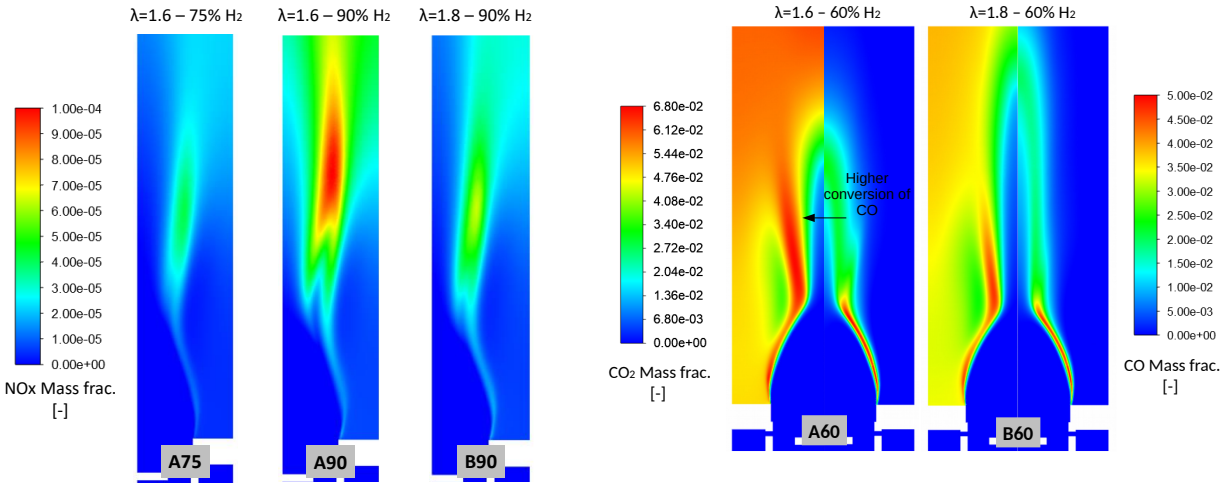

Figure 7: CFD results for: (a) NO_x formation rates and (b) CO_2 and CO mass fractions

The CO concentrations presented relatively high values and increased significantly for A60 and B60 due to the higher methane concentration in the fuel. The increment at 60% H_2 was specially higher at λ =1.8 (B60). Carbon monoxide is commonly produced when combustion reactions are not fully completed, mostly due to lack of air or low mixing [47]. This may lead to think that higher λ levels might induce lower CO formation due to an increasing oxygen presence that could oxidise the intermediate CO. However, lower λ led to a larger combustion zones (in case of higher hydrogen concentrations a post flame shear layer appeared). This can be observed through the temperature contours at A60 and B60. As concluded by [32], the enlarged combustion zone favour the CO oxidation to CO_2, reducing the overall CO emissions. This effect can be appreciated in Figure 7 (b), where CO and CO_2 concentrations for A60 and B60 are compared, showing higher CO conversion across the reacting zone at A60. However, this effect had a negative impact on NO_x formation, prompted by the higher temperatures and residence times of the NO_x precursors. Thus, further optimisations should be considered to deal with the combination of this phenomena in order to reach a compromise.

Hence, numerical results showed that the present burner geometry would be able to work without fuel jet penetration at H_2-60%, demonstrating that the initial burner geometry dimensions would determine the fuel flexibility of the micromix burner. In the light of the present results and in contrast to the fuel flexibility of micromix gas turbines, the employed geometry at industrial-scale burner conditions showed a low fuel flexibility due to its high impact on the momentum flux ratios. Likewise, NO_x emissions were doubled at λ =1.6 for the considered fuel mixtures. Contrarily, CO emissions were halved at λ =1.6 for hydrogen content of 60%. As observed, the higher the hydrogen content the lower the impact on CO reduction when decreasing λ (CO emissions increased from B90 to A90). Thus, reducing the λ could be a good strategy to further reduce the CO emissions at H_2-60% or lower concentrations, as long as the limit of the low NO_x is

note exceeded. However, this would reduce the fuel flexibility.

It can be concluded that the discussed numerical outcomes served as an initial baseline study, showing a potential for further burner optimisations for higher fuel flexibility together with low NO_x and CO concentrations. However, it is clear that flexibility would be limited under industrial-scale burner conditions since working at lower λ constrains the turbulence level and the performance of the fuel-air mixing against the lean nature of micromix gas turbines with λ values up to λ=2.5, where good flexibility of hydrogen/natural gas blends has already been demonstrated [33].

6. Conclusions

The present study lays the groundwork for future research into the usage of H_2/CH_4 blends in micromix burners for industrial combustion systems. Based on the scaling methodology presented at Ref.[17] and the experimental validation with pure hydrogen, it was decided to study the impact of H_2/CH_4 blends. For that purpose, similar modelling approach was selected, including improved combustion modelling through the EDC combustion model instead of the FGM model. The EDC model has the advantage of solving the transport equations for all species, and although it increases the computational cost considerably, it offers more reliable results. Despite the good predictions of thermal NO_x using the FGM model in our previous work [17], the present calculations were conducted with the EDC model, since the simulations with H_2/CH_4 blends have not been validated at the present stage. Therefore, in order to reduce the uncertainties in the predictions, a more robust combustion model was necessary.

CFD simulations for varying hydrogen concentrations (90, 75 and 60 %) and air-fuel ratios (λ =1.8 and 1.6) showed that jet penetration occurs for hydrogen concentrations above 60 % in the fuel. Furthermore NO_x formation increased significantly for λ =1.6 due to the post-shear layer NO_x formation phenomena. Concerning the CO emissions, results at λ =1.6 showed lower concentrations than for λ =1.8 at 60%/H_2, concluding that the larger combustion zones at λ =1.6 favoured the CO oxidation process across the flame. This CO reduction effect was reduced at 75%/H_2 and dumped at 90%/H_2. Hence, using a lower λ could be a good strategy to further reduce the CO emissions at H_2-60% or lower concentrations, as long as the limit of the low NO_x is note exceeded. Nevertheless, this would also reduce the fuel flexibility to work with higher hydrogen content in the fuel.

Overall, despite NO_x values were maintained low, fuel jet penetration and CO emissions showed opposite trends. Hence, it can be concluded that the present results demonstrated low fuel flexibility for the considered burner geometry and industrial-scale operating conditions. This could be mainly attributed to the lower λ, which were reduced from λ =2.5 (in gas turbine conditions) to λ =1.6 and 1.8, increasing the momentum flux ratio and therefore promoting the fuel jet penetration for out-design points at 75%/H_2 and 90%/H_2. Working with higher λ levels gives the possibility of increasing the air mass flux for higher H_2 concentrations in the fuel in order to keep the momentum flux ratio low enough according to equation (9). Therefore, if it were possible to work with a wider λ range, the flexibility to use blends in the present micromix burner would be greater. Finally, future work would include geometry optimisation and it will be necessary to adapt the experimental setup to validate the mixtures under the new geometries. It will also be necessary to analyse the efficiency of the combustion process taking into account the heat exchanger.

Acknowledgements

The first author's work has been funded by the Provincial Council of Bizkaia within the Technology Transfer Programme 2021, co-financed by EGEF, Basque Government, Spain; by the Elkartek project EXPERTIA (KK-2021/000 48), by the BERC 2022–2025 program, Basque Govern- ment, Spain, by the Spanish State Research Agency through BCAM Severo Ochoa excellence accreditation CEX2021-001142-S/MICIN/AEI/10.13039/501100011033. And finally, thanks to be given to the Research Group: IT1514-19.

References

[1] Z. Abdin, A. Zafaranloo, A. Rafiee, W. Mérida, W. Lipiński, K. R. Khalilpour, Hydrogen as an energy vector, Renewable and Sustainable Energy Reviews 120 (November 2019) (2020). doi:10.1016/j.rser.2019.109620.

[2] Z. Guo, W. Wei, L. Chen, X. Zhang, S. Mei, Equilibrium model of a regional hydrogen market with renewable energy based suppliers and transportation costs, Energy 220 (2021) 119608. doi:https://doi.org/10.1016/j.energy.2020.119608.

[3] C. J. Quarton, S. Samsatli, Power-to-gas for injection into the gas grid: What can we learn from real-life projects, economic assessments and systems modelling?, Renewable and Sustainable Energy Reviews 98 (August) (2018) 302–316. doi:10.1016/j.rser.2018.09.007.
URL https://doi.org/10.1016/j.rser.2018.09.007

[4] A. Ajanovic, A. Glatt, R. Haas, Prospects and impediments for hydrogen fuel cell buses, Energy 235 (2021) 121340. doi:https://doi.org/10.1016/j.energy.2021.121340.

[5] J. Luo, Z. Liu, J. Wang, H. Xu, Y. Tie, D. Yang, Z. Zhang, C. Zhang, H. Wang, Investigation of hydrogen addition on the combustion, performance, and emission characteristics of a heavy-duty engine fueled with diesel/natural gas, Energy 260 (2022) 125082. doi:https://doi.org/10.1016/j.energy.2022.125082.

[6] P. Miranda, Science and Engineering of Hydrogen-Based Energy Technologies: Hydrogen Production and Practical Applications in Energy Generation, Elsevier Science, 2018.

[7] J. E, Y. Mei, C. Feng, J. Ding, L. Cai, B. Luo, A review of enhancing micro combustion to improve energy conversion performance in micro power system, International Journal of Hydrogen Energy 47 (53) (2022) 22574–22601. doi:https://doi.org/10.1016/j.ijhydene.2022.05.042.

[8] N. Fitzpatrick, T. Parrique, I. Cosme, Exploring degrowth policy proposals: A systematic mapping with thematic synthesis, Journal of Cleaner Production 365 (2022) 132764. doi:https://doi.org/10.1016/j.jclepro.2022.132764.

[9] D. H. Meadows, D. L. Meadows, J. Randers, W. W. Behrens III, The limits to growth, Universe Books, 1972.

[10] The European Commission, European Clean Hydrogen Alliance, The European Commission, 2020.
URL https://single-market-economy.ec.europa.eu/industry/strategy/industrial-alliances/european-clean-hydrogen-alliance_en

[11] X. Yang, T. Wang, Y. Zhang, H. Zhang, Y. Wu, J. Zhang, Hydrogen effect on flame extinction of hydrogen-enriched methane/air premixed flames: An assessment from the combustion safety point of view, Energy 239 (2022) 122248. doi:https://doi.org/10.1016/j.energy.2021.122248.

[12] X. Zhan, Z. Chen, C. Qin, Effect of hydrogen-blended natural gas on combustion stability and emission of water heater burner, Case Studies in Thermal Engineering 37 (2022) 102246. doi:https://doi.org/10.1016/j.csite.2022.102246.

[13] H. Yilmaz, I. Yilmaz, Flame and instability characteristics of high hydrogen content gas mixtures, Energy 223 (2021) 120084. doi:https://doi.org/10.1016/j.energy.2021.120084.

[14] M. Ditaranto, T. Heggset, D. Berstad, Concept of hydrogen fired gas turbine cycle with exhaust gas recirculation: Assessment of process performance, Energy 192 (2020) 116646. doi:https://doi.org/10.1016/j.energy.2019.116646.

[15] M. Ozturk, I. Dincer, System development and assessment for green hydrogen generation and blending with natural gas, Energy 261 (2022) 125233. doi:https://doi.org/10.1016/j.energy.2022.125233.

[16] J. Bard, G. Norman, P. Selzam, M. Beil, B. M. Wiemer, M, The limitations of hydrogen blending in the european gas grid, Fraunhofer Institute for Energy Economics and Energy System Technology (IEE) (2022).

[17] G. Lopez-Ruiz, I. Alava, J. Blanco, Study on the feasibility of the micromix combustion principle in low nox h2 burners for domestic and industrial boilers: A numerical approach, Energy 236 (2021) 121456. doi:https://doi.org/10.1016/j.energy.2021.121456.

[18] B. E. Gelfand, M. V. Silnikov, S. P. Medvedev, S. V. Khomik, Thermo-Gas Dynamics of Hydrogen Combustion and Explosion, springer, 2012.

[19] J. Warnatz, U. Maas, R. W. Dibble, R. W. Dibble, Combustion: Physical and Chemical Fundamentals, Modelling and Simulation, Experiments, Pollutant Formation., Springer, 2001.

[20] S. McAllister, J. Y. Chen, A. C. Fernandez-Pello, Fundamentals of Combustion Processes, Mechanical Engineering Series, Springer New York, 2011.

[21] G. Lopez-Ruiz, I. Alava, I. Urresti, J. M. Blanco, B. Naud, Experimental and numerical study of NOx formation in a domestic H2/air coaxial burner at low Reynolds number, Energy 221 (2021) 119768. doi:https://doi.org/10.1016/j.energy.2021.119768.

[22] A. H. Ayed, K. Kusterer, H. H. Funke, J. Keinz, D. Bohn, CFD based exploration of the dry-low-NOx hydrogen micromix combustion technology at increased energy densities, Propulsion and Power Research 6 (1) (2017) 15–24. doi:10.1016/j.jppr.2017.01.005.

[23] H. H. Funke, N. Beckmann, S. Abanteriba, An overview on dry low NO x micromix combustor development for hydrogen-rich gas turbine applications, International Journal of Hydrogen Energy 44 (13) (2019) 6978–6990. doi:10.1016/j.ijhydene.2019.01.161.

[24] N. Tekin, M. Ashikaga, A. Horikawa, D.-I. H. Funke, Enhancement of fuel flexibility of industrial gas turbines by development of innovative hydrogen combustion systems (2019).

[25] CORDIS — European commission. (2018). Enabling cryogenic Hydrogen based CO2 free air transport (ENABLE H2) — Projects — H2020 — CORDIS — European commission.

[26] X. Sun, V. Sethi, Enabling Cryogenic Hydrogen-Based CO2-free Air Transport (ENABLEH2) – Micromix Combustion Research (2019).

[27] R. B. Abdallah, NOx Micromix Hydrogen Combustion System: -Preliminary Design and Performance Assesment of Novel Injectors Using RANS and LES CFD, Tech. rep., Cranfield University (2017).

[28] V. Zangeneh, A. Alipoor, Stability study of hydrogen-air flame in a conical porous burner, Energy 215 (2021) 119140. doi:https://doi.org/10.1016/j.energy.2020.119140.
[29] M. Mayrhofer, M. Koller, P. Seemann, R. Prieler, C. Hochenauer, Assessment of natural gas/hydrogen blends as an alternative fuel for industrial heat treatment furnaces, International Journal of Hydrogen Energy 46 (41) (2021) 21672–21686. doi:https://doi.org/10.1016/j.ijhydene.2021.03.228.
[30] S. Rahimi, K. Mazaheri, A. Alipoor, A. Mohammadpour, The effect of hydrogen addition on methane-air flame in a stratified swirl burner, Energy 265 (2023) 126354. doi:https://doi.org/10.1016/j.energy.2022.126354.
[31] T. B. Kıymaz, E. Böncü, D. Güleryüz, M. Karaca, B. Yılmaz, C. Allouis, İskender Gökalp, Numerical investigations on flashback dynamics of premixed methane-hydrogen-air laminar flames, International Journal of Hydrogen Energy 47 (59) (2022) 25022–25033. doi:https://doi.org/10.1016/j.ijhydene.2022.05.230.
[32] N. Beckmann, Characterization of the Hydrogen-Dry-Low-NOx-Micromix- Combustion Principle for Hydrogen-Methane Fuel Mixtures, Ph.D. thesis (2019).
[33] N. Tekin, M. Ashikaga, F. H. Horikawa, A, Enhancement of fuel flexibility of industrial gas turbines by development of innovative hydrogen combustion systems, Gas for energy (2018).
[34] H. H. Funke, N. Beckmann, J. Keinz, S. Abanteriba, Comparison of Numerical Combustion Models for Hydrogen and Hydrogen-Rich Syngas Applied for Dry-Low-NOx-Micromix-Combustion, Proceedings of ASME Turbo Expo (2016).
[35] J. Chacón, J. M. Sala, J. M. Blanco, Investigation on the design and optimization of a low NOx - CO emission burner both experimentally and through computational fluid dynamics (CFD) simulations, Energy and Fuels 21 (1) (2007) 42–58. doi:10.1021/ef0602473.
[36] C. E. B. Jr., Industrial Burners Handbook, Industrial Combustion, CRC Press, 2003.
[37] F. R. Menter, Two-equation eddy-viscosity turbulence models for engineering applications, AIAA Journal 32 (8) (1994) 1598–1605. doi:10.2514/3.12149.
[38] G. Babazzi, P. Q. Gauthier, P. Agarwal, J. McClure, V. Sethi, NOx emissions predictions for a hydrogen micromix combustion system, Proceedings of the ASME Turbo Expo 3 (2019). doi:10.1115/GT2019-90532.
[39] P. Agarwal, X. Sun, P. Q. Gauthier, V. Sethi, Injector design space exploration for an ultra-low NOx hydrogen micromix combustion system, Proceedings of the ASME Turbo Expo 3 (2019). doi:10.1115/GT2019-90833.
[40] W. Han, A. Scholtissek, F. Dietzsch, C. Hasse, Thermal and chemical effects of differential diffusion in turbulent non-premixed h2 flames, Proceedings of the Combustion Institute 38 (2) (2021) 2627–2634. doi:https://doi.org/10.1016/j.proci.2020.06.049.
[41] N. Klarmann, B. T. Zoller, T. Sattelmayer, Numerical modeling of co-emissions for gas turbine combustors operating at part-load conditions, Journal of the Global Power and Propulsion Society 2 (2018) 376–387. doi:10.22261/JGPPS.C3N5OA.
[42] Modeling CO With Flamelet-Generated Manifolds: Part 1—Flamelet Configuration, Vol. Volume 2: Combustion, Fuels and Emissions, Parts A and B of Turbo Expo: Power for Land, Sea, and Air. doi:10.1115/GT2012-69528.
[43] B. B. F. Magnussen, The Eddy Dissipation Concept: A Bridge Between Science and Technology, ECCOMAS Thematic Conference on Computational Combustion (2005) 1–25.
URL http://folk.ntnu.no/ivarse/edc/BFM{_}ECOMAS2005{_}Lisboa.pdf
[44] A. De, E. Oldenhof, P. Sathiah, D. Roekaerts, Numerical simulation of delft-jet-in-hot-coflow (djhc) flames using the eddy dissipation concept model for turbulence–chemistry interaction, Flow, Turbulence and Combustion 87 (2011) 537–567. doi:10.1007/s10494-011-9337-0.
[45] A. Kazakov, M. Frenklach, Tech. rep., http://combustion.berkeley.edu/drm/.
[46] ANSYS Fluent Inc. 2020 R1, documentation user's guide. (2020).
[47] E. K. Vakkilainen, 2 - solid biofuels and combustion, in: E. K. Vakkilainen (Ed.), Steam Generation from Biomass, Butterworth-Heinemann, 2017, pp. 18–56. doi:https://doi.org/10.1016/B978-0-12-804389-9.00002-2.